Supplementary material

Table S1. Additional information about the skeletal samples, including the institution in which the remains are curated.

Population	Details	Institution[a]
Ainu	Recent, probably 18th-19th century AD	KU, TU
Alaska	The Tigara burials represent protohistoric/historic whale hunters (circa 13th-18th century AD). The Ipiutak people (circa 4th-9th century AD) appear to have been caribou hunters.	AMNH
Arikara	Larson Site, South Dakota (1,675-1,780 AD).	UTK
Austria	Early 20th century AD immigrants to the USA from Bohemia (CMNH) and Austrian remains from the 19th century AD (NM).	CMNH, NM
Botswana	Tswana remains of cadaveric origin, Raymond Dart collection, 19th century AD.	UW
California	Native Californians from two prehistoric sites: Ala-329 and CC-138. CCo-138, also called Hotchkiss site, is located 3 miles from the town of Oakley. The burials date from the Late Period (1,500-1,750 AD). The Ala-329 site, also called Ryan Mound site, is located in Alameda County on the southeastern side of the San Francisco Bay. It dates to the Middle and Late Periods (500-1,750 AD), but the large majority of the remains date to after 1,000 AD.	UCB
Egypt	The sample includes the El Hesa material (American Museum of Natural History), dated to the 4th-7th century AD, and the undated El Gizeh material (Naturhistorisches Museum, Wien).	AMNH, NM
France	French remains of cadaveric origin, 20th century AD, mostly middle age or older.	MdH
Fuegian	Mostly undated remains, but likely all from the 19th century AD.	MNdAE, UR
India	Probably recent, 19th-20th century AD; they were bought by the Museum of Man from a provider of human remains for anatomical collections.	MoM
Iran	Hasan-lu site, 9th century BC.	UP
Italy	Early 20th century AD immigrants to the USA from Italy (CMNH), and recent Italian remains (prob. 19th century AD) from an Italian anatomical collection (MNdAE).	CMNH, MNdAE
Japan	Recent Japanese, probably all 20th century AD.	KU, MdH
Kenya	Kykuyu remains from the 20th century AD.	NMK
KhoeSan	Human remains spanning a wide period of time, from relatively recent (19th-20th century AD) to the first centuries BC. Mostly undated.	MGM, NHM, UW

Lesotho	Sotho remains of cadaveric origin, Raymond Dart collection, 19th century AD.	UW
Nubia	Necropolis of Sayala, 3rd-4th century AD.	NM
Patagonia	Mostly undated remains, but likely from the 19th century AD.	MdH, MNdAE
Peru	Undated pre-Columbian remains from the ancient necropolis of Ancon.	MdH
Philippines	Undated, but probably all recent (18th-19th century AD). Coded as "negritos" or Aeta in the museum's catalogue.	MdH
Portugal	Recent remains (19th century and early 20th century AD) from the Cemitério da Conchada in Coimbra.	CU
Sadlermiut	Sadlermiut remains from Native Point and Prairie Point, probably 16th-19th century AD.	MCC
Swaziland	Swazi remains of cadaveric origin, Raymond Dart collection, 19th century AD.	UW
Thailand	Modern remains of cadaveric origin (20th and 21st century AD).	CMU, MdH

[a]*(AMNH = American Museum of Natural History, New York, USA; CMNH = Cleveland Museum of Natural History, Ohio, USA; CMU = Chiang Mai University, Thailand; CU = Coimbra University, Portugal; KU = Kyoto University, Japan; MCC = Musée Canadien des Civilisations, Gatineau, Canada; MdH = Musée de l'Homme, Paris, France; MGM = McGregor Museum, Kimberley, South Africa; MNdAE = Museo Nazionale di Antropologia e Etnologia, Firenze, Italy; MoM = San Diego Museum of Man, California, USA; NHM = Natural History Museum, London, UK; NM = Naturhistorisches Museum, Wien, Austria; NMK = National Museum of Kenya, Nairobi, Kenya; TU = Tokyo University, Japan; UCB = University of California at Berkeley, USA; UP = University of Pennsylvania at Philadelphia, USA; UR = University of Rome "La Sapienza", Italy; UTK = University of Tennessee at Knoxville, USA; UW = University of Witwatersrand, Johannesburg, South Africa).*

Table S2. Coordinates and climatic data for the populations under study.

Population	Longitude	Latitude	Min. temperature (°C)	Max. temperature (°C)
Ainu	142.70	43.33	-16.5	20.7
Alaska	-166.80	68.33	-26.7	10.3
Arikara	-100.07	43.95	-15.0	32.4
Austria	14.55	47.52	-10.1	17.0
Botswana	23.92	-22.05	5.0	33.2
California	-122.00	38.20	3.1	30.0
Egypt	31.22	30.03	6.9	34.9
France	2.35	48.85	0.8	24.8
Fuegian	-71.28	-53.50	-2.6	12.2
India	88.45	22.58	12.6	35.9
Iran	51.42	35.67	-5.0	36.0
Italy	12.42	41.88	3.8	30.0
Japan	138.25	36.20	-7.9	28.1
Kenya	38.00	1.00	15.6	33.9
KhoeSan	21.00	-25.00	1.5	34.9
Lesotho	28.23	-29.62	-2.7	23.7
Nubia	30.22	12.85	14.0	38.7
Patagonia	-69.00	-41.75	-6.2	22.6
Peru	-74.62	-12.77	-1.5	18.4
Philippines	121.77	12.87	22.6	32.6
Portugal	-8.43	40.22	5.1	28.1
Sadlermiut	-84.67	64.00	-34.5	13.8
Swaziland	31.47	-26.52	8.1	29.3
Thailand	99.00	18.78	12.8	36.0

Table S3. Matching skeletal and genetic samples. Number of individuals of the genetic sample is also reported.

Skeletal samples	Genetic samples	N
Alaska	Chukchi, Naukan, Koryak from Russia	42
Arikara	Algonquin from Canada	9
Austria	Hungarian	10
Botswana	Tswana + South African Tswana	7
California	Pima from Mexico	14
Egypt	Egypt	18
France	France + South France	32
Fuegians + Patagonia	Chilote	4
India	Gujarati (A, B, C, D), Kharia, Lodhi, Mala, Onge, Tiwari, Vishwabrahmin	97
Iran	Iran	8
Italy	Italians from East and West Sicily, Bergamo and Tuscany	31
Japan	Japanese	29
Kenya	Kikuyu	4
KhoeSan	Nama and Xuun	29
Portugal	Spanish from Andalucia, Extremadura, Galicia	14
Sadlermiut	Chukchi, Naukan, Koryak from Russia	42
Thailand	Thai	10

Table S4. Significance of post-hoc Tukey tests comparing canal shape in different geographic regions. Significant results in bold.

INLET	Americas	Asia	Europe & North Africa
Asia	**<0.001**		
Europe & North Africa	**0.003**	**0.011**	
Sub-Saharan Africa	**<0.001**	0.465	**<0.001**
MIDPLANE	Americas	Asia	Europe & North Africa
Asia	**<0.001**		
Europe & North Africa	0.751	**0.023**	
Sub-Saharan Africa	**<0.001**	0.980	**0.005**
OUTLET	Americas	Asia	Europe & North Africa
Asia	**<0.001**		
Europe & North Africa	0.970	**0.003**	
Sub-Saharan Africa	**<0.001**	0.076	**<0.001**

Table S5. Coefficient of variation (CV) of the three birth canal indices and raw diameters, compared with indices and raw measurements from other anatomical regions calculated from the Goldman dataset (http://web.utk.edu/~auerbach/GOLD.htm; [2]). Only female individuals were included in the analyses.

Indices	**CV**	**Indices**	**CV**
Inlet	9.936	Brachial index	4.392
Midplane	9.884	Crural index	3.215
Outlet	11.767	Pelvic breadth / femoral length	6.707
Raw measurements	**CV**	**Raw measurements**	**CV**
Inlet AP	8.362	Humerus max length	5.753
Inlet ML	7.753	Radius max length	6.447
MidplaneAP	7.166	Femur max length	5.688
Midplane ML	9.156	Tibia max length	6.727
Outlet AP	7.817	Bi-iliac breadth	6.669
Outlet ML	10.261		

Table S6. Results of the Mantel tests between population canal shape differences (Q) and climatic distances (Tmin.d and Tmax.d, respectively distance matrices based on minimum temperature and maximum temperature). The values obtained after correcting for genetic distance (G) are also reported. The reduced dataset for which genetic data were available was used for these analyses.

Model	**R^2**	**P-value**
Q VS Tmin.d	0.045	0.095
Q VS Tmax.d	0.020	0.136
Q VS Tmin.d / G	0.019	0.168
Q VS Tmax.d / G	0.016	0.153

Table S7. Results of the Mantel tests between population differences in canal indices and climatic distances (Tmin.d and Tmax.d, respectively distance matrices based on minimum temperature and maximum temperature). The values obtained after correcting for genetic distance (G) are also reported. The reduced dataset for which genetic data were available was used for these analyses. Significant results in bold.

Model	R^2	P-value	Model	R^2	P-value
Inlet VS Tmin.d	0.153	**0.002**	Inlet VS Tmin.d / G	0.124	**0.006**
Inlet VS Tmax.d	0.063	**0.024**	Inlet VS Tmax.d / G	0.061	**0.026**
Midplane VS Tmin.d	0.031	0.099	Midplane VS Tmin.d / G	0.029	0.113
Midplane VS Tmax.d	0.003	0.279	Midplane VS Tmax.d / G	0.003	0.292
Outlet VS Tmin.d	<0.001	0.405	Outlet VS Tmin.d / G	0.007	0.702
Outlet VS Tmax.d	0.001	0.348	Outlet VS Tmax.d / G	<0.001	0.435

Table S8. Estimation of the inlet, midplane and outlet indices in extinct hominin fossils (suggested to be females) of the Homo and Australopithecus genera, and modern human range of variation estimated from this study. The data are drawn from published studies, and some refer to alternative reconstructions of the same fossil.

Species	Fossil	Reference	Inlet (AP/ML)	Midplane (AP/ML)	Outlet (AP/ML)
H. sapiens		This study	0.63-1.17	0.97-1.63	0.74-1.47
H. neanderthalensis	Tabun C1	[3]	0.75-0.85	1.07-1.24	0.98-1.16
H. neanderthalensis	Tabun C1	[4]	0.79		0.70
H. heidelbergensis?	SH1	[5]	0.79	1.23	0.94
H. heidelbergensis?	SH1	[6]	0.78	1.09	0.95
H. erectus?	BSN49/P27	[7]	0.79	0.97	
A. sediba	MH2	[8]	0.69		
A. africanus	Sts 14	[9]	0.88	0.97	0.79
A. africanus	Sts 14	[10]	0.71	0.79	
A. africanus	Sts 65	[11]	0.82		
A. afarensis	AL 288-1	[12]	0.62	0.91	1.01
A. afarensis	AL 288-1	[13]	0.58	0.71	0.74
A. afarensis	AL 288-1	[9]	0.66	1.09	1.11

References

1 Kurki, H. K. Protection of obstetric dimensions in a small-bodied human sample. *American Journal of Physical Anthropology* **133**, 1152-1165 (2007).

2 Auerbach, B. M. & Ruff, C. B. Limb bone bilateral asymmetry: variability and commonality among modern humans. *J. Hum. Evol.* **50**, 203-218 (2006).

3 Ponce de León, M. S. *et al.* Neanderthal brain size at birth provides insights into the evolution of human life history. *Proc. Natl Acad. Sci. USA* **105**, 13764-13768 (2008).

4 Weaver, T. D. & Hublin, J. J. Neandertal birth canal shape and the evolution of human childbirth. *Proc. Natl Acad. Sci. USA* **106**, 8151-8156 (2009).
5 Arsuaga, J.-L. *et al.* A complete human pelvis from the Middle Pleistocene of Spain. *Nature* **399**, 255-258 (1999).
6 Bonmatí, A. *et al.* Middle Pleistocene lower back and pelvis from an aged human individual from the Sima de los Huesos site, Spain. *Proc. Natl Acad. Sci. USA* **107**, 18386-183 (2010).
7 Simpson, S. W. *et al.* A female *Homo erectus* pelvis from Gona, Ethiopia. *Science* **322**, 1089-1092 (2008).
8 Kibii, J. M. *et al.* A partial pelvis of *Australopithecus sediba*. *Science* **333**, 1407-1411 (2011).
9 Häusler, M. & Schmid, P. Comparison of the pelves of Sts 14 and AL288-1: implications for birth and sexual dimorphism in australopithecines. *J. Hum. Evol.* **29**, 363-383 (1995).
10 Berge, C. & Goularas, D. A new reconstruction of Sts 14 pelvis (*Australopithecus africanus*) from computed tomography and three-dimensional modeling techniques. *J. Hum. Evol.* **58**, 262-272 (2010).
11 Claxton, A. G., Hammond, A. S., Romano, J., Oleinik, E. & DeSilva, J. M. Virtual reconstruction of the *Australopithecus africanus* pelvis Sts 65 with implications for obstetrics and locomotion. *J. Hum. Evol.* **99**, 10-24 (2016).
12 Schmid, P. Eine Rekonstruktion des Skelettes von A.L. 288-1 (Hadar) und deren Konsequenzen. *Folia Primatol.* **40**, 283-306 (1983).
13 Tague, R. G. & Lovejoy, C. O. The obstetric pelvis of A.L. 288-1 (Lucy). *J. Hum. Evol.* **15**, 237-255 (1986).

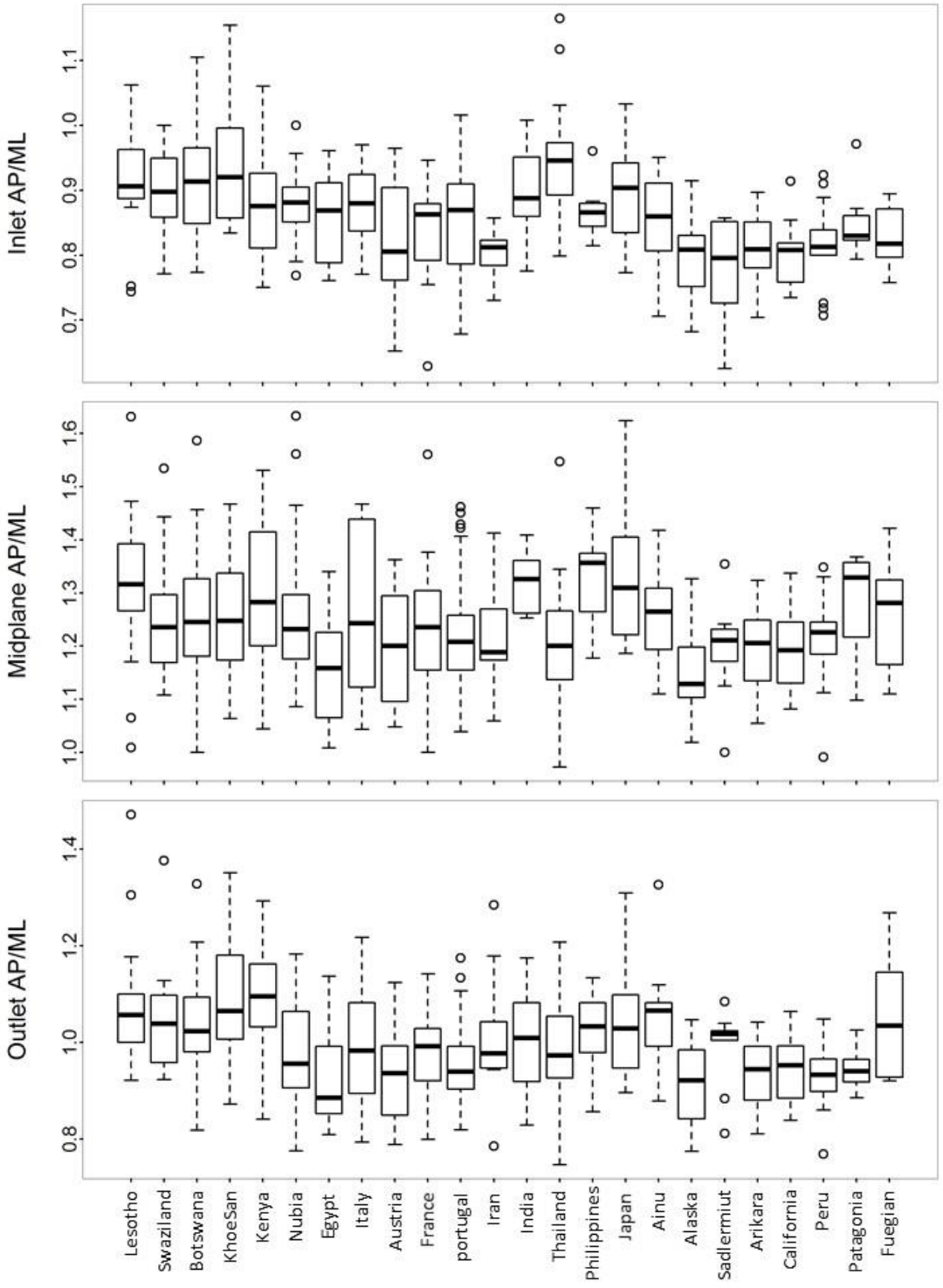

Figure S1: Variation in the inlet, midplane and outlet indices in the studied populations, arranged by increasing distance from central sub-Saharan Africa (from left to right). The boxes represent the interquartile distance, the whiskers extend to the most extreme data point which is no more than 1.5 times the interquartile range, and outliers are highlighted as open circles.

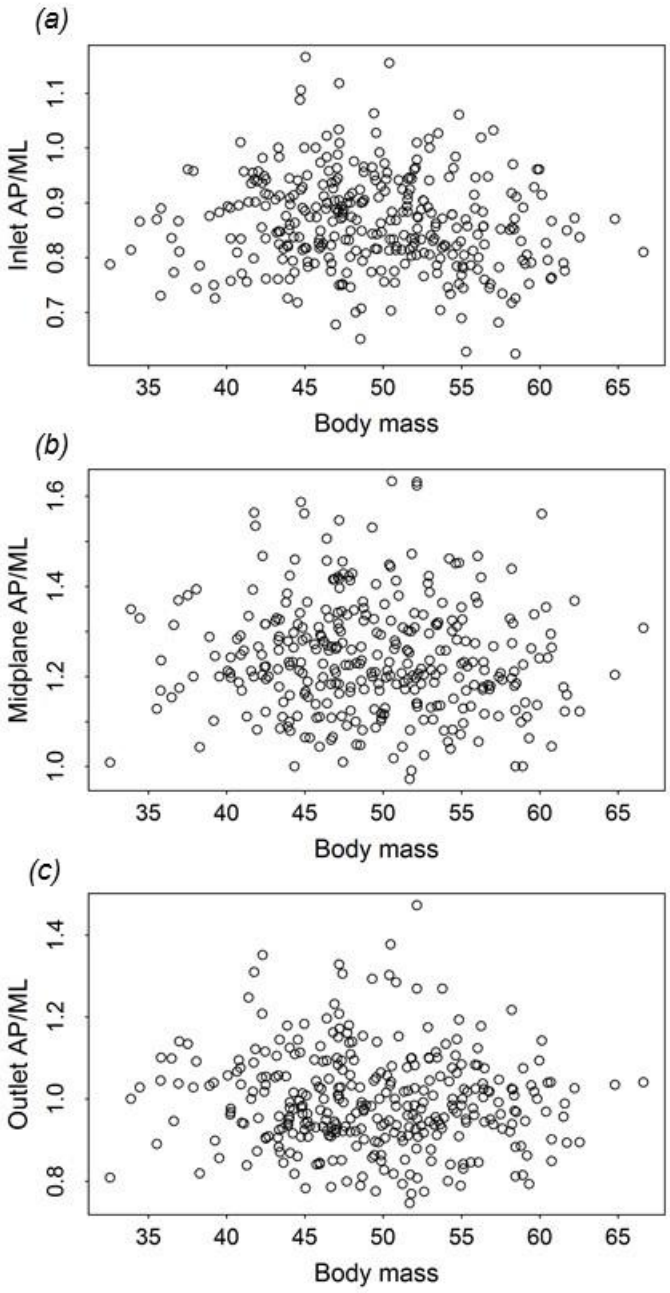

Figure S2. Plots of individual canal indices against body size: (*a*) inlet; (*b*) midplane; (*c*) outlet.